Modelling water trap seal boundary conditions in building drainage systems

Building Services Engineering
Research and Technology

Modelling water trap seal boundary conditions in building drainage systems: CFD analysis of unsteady friction to improve accuracy

Journal:	*Building Services Engineering Research and Technology*
Manuscript ID	BSE-C-16-080.R2
Manuscript Type:	Research Paper
Date Submitted by the Author:	13-May-2017
Complete List of Authors:	Jean, Nicole; Mace Group Gormley, Michael; Heriot-Watt University, The Water Academy
Keywords:	Water trap seal, Modelling, CFD modelling, Building Drainage

Abstract:	The water trap seal in building drainage systems remains the sole barrier between the public sewer network and habitable space inside a building. AIRNET, a 1-D Method of Characteristics based model, enables rapid whole system testing, however the present boundary condition for the water trap seal within the model is based solely on steady state conditions, ignoring system dynamics. CFD offers an opportunity to numerically evaluate the flow patterns within the trap seal in response to applied air pressure transients. This research confirms the importance of the rate of rise, and hence frequency, of air pressure transients incident on water trap seals and relates this to potential vulnerabilities of different device geometries, particularly the ratio between inner and outer wall length. The research led to the development of a dynamic velocity decrement model encapsulating unsteady friction and separation losses linked to device geometry for the first time. The development of a frequency dependent internal energy term Δv, suitable for inclusion in AIRNET provides the capability to predict more realistic water trap response to air pressure transients over a range of air pressure transient frequencies likely to cause problems: 1Hz to 8Hz.

Modelling water trap seal boundary conditions in building drainage systems: CFD analysis of unsteady friction to improve accuracy

N. J. Jean PhD

Public Health Design Engineer, Mace, 155 Moorgate, London, UK

Email: Nicole.Jean@macegroup.com

M. Gormley PhD CENG MCIBSE

Associate Professor, The Water Academy, Heriot Watt University, Edinburgh, UK

Email: M.Gormley@hw.ac.uk

Abstract

The safe removal of disease carrying human waste is the objective of all sanitation systems and the limiting of air pressure transients within the system remains a significant part of current codes and regulations. The water trap seal offers fundamental protection and is the system's sole barrier between the public sewer network and habitable space inside a building. Modelling water trap seal responses to air pressure fluctuations offers an opportunity to analyse whole system performance, but the quality of the data depends on the accuracy of the modelling technique and that of the defining inputs. AIRNET, a 1-D Method of Characteristics based model, enables rapid whole system testing, however the present boundary condition for the water trap seal within the model is based solely on steady state conditions, ignoring system dynamics. CFD offers an opportunity to numerically evaluate the flow patterns within the trap seal in response to applied air pressure transients. This research confirms the importance of the rate of rise, and hence frequency, of air pressure transients incident on water trap seals and relates this to potential vulnerabilities of different device geometries, particularly the ratio between inner and outer wall length. The research led to the development of a dynamic velocity decrement model encapsulating unsteady friction and separation losses

linked to device geometry for the first time. The development of a frequency dependent internal energy term Δv, suitable for inclusion in AIRNET provides the capability to predict more realistic water trap response to air pressure transients over a range of air pressure transient frequencies likely to cause problems: 1Hz to 8Hz.

Practical Application

Whole system modelling can greatly improve the ability of design engineers to fully simulate the operation of a building drainage system in a realistic way. The work described in this paper improves the accuracy of whole system models by evaluating water dynamic responses to air pressure transients using a range of techniques including CFD and more traditional 1-D finite difference method of characteristics models. The work also paves the way for more robust evaluation of building drainage products through in-depth investigation of the fluid mechanics associated with their operation.

Nomenclature

A	Acceleration
C	Acoustic velocity
c	Wave speed
C	Y intercept
C_L	Length relationship Y intercept
C_0	Local acoustic velocity
C_R	Boundary reflection coefficient
C^+	Characteristic slope
C^-	Characteristic slope
D	Internal pipe diameter
D_h	Hydraulic diameter
d	Distance from inner surface of bend
f	Friction factor
H	Trap fluid height
i	Distance factor

k	Separation loss coefficient
L	Pipe length
L_i	Inner length of bend
L_o	Outer length of bend
m	hydraulic mean depth
n	number of pipes, nodes or selected points along a plane
P	Wetted perimeter
p	Pressure
ρ	Density of the fluid
Q	Volumetric flow rate
Re	Reynold's number
r^n	Residual error
S_v	Slope of velocity plot
S_o	Slope of pipe
T	Threshold

t	Time
t^*	Non-dimensional time
Δt	Time increment
V	Mean velocity
V_{mf}	Mean velocity across applied frequency
V_w	Liquid column velocity
v	Fluid velocity
Δv	Frequency dependant change in velocity
x	Position / distance

Subscript

A, B, C, R, S	Nodes with known values of *p,c,u* at time *t*
atm	Atmospheric conditions
av	Average
L	Length relationship descriptor
Max	Maximum values

Trap	Trap conditions
w	Water flow

Other

C_μ	Dimensionless constant
μ	Fluid viscosity
μ_k	Kinematic viscosity
μ_t	Turbulent viscosity
τ	Viscous stresses
γ	Ratio of specific heat at constant pressure to constant volume
Ø	Diameter
λ	Ratio of specific heat at constant pressure to volume

Abbreviations

AAV – Air Admittance Valve

BC- Boundary condition

BDS – Building Drainage System

CEL - CFX expression language

CFD – Computational Fluid Dynamics

D – Dimension

Eq - Equation

FD – Finite Difference

FDM- Finite Difference Method

FE – Finite Element

FEM – Finite Element Method

FV – Finite Volume

FVM – Finite Volume Method

HHD- Hybrid hard drive

MoC – Method of Characteristics

PDE – Partial differential equations

SARS – Severe Acute Respiratory Syndrome

VF – Volume fraction

VOF – Volume of Fluid

WHO – World Health Organisation

1 Introduction

The Severe Acute Respiratory Syndrome (SARS) outbreak in 2003 at the Amoy Gardens, highlighted the potential consequences of depleted water trap seals (U-bends) raising the possibility of disease-spread from the sewer into the building.[1,2,3,4,5]. This appliance water trap seal though sometimes altered in design, remains relatively unchanged in its operation since developed in the 18th century, and acts as the 'final defence mechanism' against the propagation of sewer gas into the indoor space.

The value of modelling water, waste movement and air inside building drainage systems (BDS) has never been greater and modelling of termination devices such as U-bends gain increased relevance since it is the interface between the main sewer system and habitable space. Current whole system models[5] represent the termination as a static device which does not respond to the dynamic forces inherent with the system.

At the centre of the difficulties surrounding the development of boundary equations from laboratory investigation is the complex distribution of frictional forces within a water trap. These frictional forces are unsteady and are not equally distributed throughout the flow area. Unsteady frictional representations for multi-phase water and air mixtures in curved conduit U-bend water traps are not well understood. The usual approach is to use the Colebrook-White relationship; however, there are limitations since it was derived from steady, fully developed flow, making its use in transient modelling problematic.

CFD modelling has been found to enhance understanding of the air/water interface and allows a more robust boundary condition to be developed. The data output from CFD simulations also allows detailed analysis of U-bend shape and geometry so that generalised conclusions on the influence of parameters such as inner and outer wall length can be considered; analysis which is extremely difficult to carry out in a laboratory.

1.1 Public health concerns

The rise of antimicrobial resistant pathogens, globalisation and the emergence of new microbes are some of the health security risks which the global public faces now and in the future. It is a fact that an individual who contracts an infectious disease in Latin America and Asia, and receives improper treatment, can present as a NHS patent here in the United Kingdom within days. Global public health is now a responsibility of all governments.

This was evident during the SARS epidemic in 2003, and more recently the Ebola outbreak in 2014-2015. These disease outbreaks killed 774 and 11,316 people respectively and had both a global and regional economic cost. The financial cost of emergency relief could otherwise be spent on mitigating the risks of disease outbreak. The implication of defective water trap seals in potential cross contamination is also of considerable concern[8,9]

1.2 Research Objectives

Current building drainage system models can provide useful air pressure, and airflow rate information to allow whole system responses to an event to be predicted and simulated. The most appropriate model uses a Method of Characteristics 1-D approach to numerically model real time responses. The main aim of such models is to simulate the impact of events on water trap seals, as retention of water in the trap is imperative to ensure safe systems.

Research by others has shown that water trap seals respond differently to air pressure transients with different rise times.[5]

The objectives of this research can be summarised as follows:

Develop a methodology for the evaluation of transient flow friction representation using a commercially available CFD program – ANSYS CFX, to establish a boundary condition for a water trap seal, which incorporates a frequency dependent representative of friction suitable for inclusion in a MoC 1-D model – AIRNET and validate.

2 Frictional representation of flow in the water trap seal

Friction, in the context of a curved pipe U-bend water trap seal represents the resistance to motion caused by the shear stress between the fluid and the pipe wall surface.

Traditionally, this friction is assumed to be steady and uniform. Early research in the representation of friction in unsteady flow in conduits was conducted by Carstens and Roller[10], Zilke[11] and more recently by Vitkovsky *et al*[12]. Carstens and Roller developed an additional empirical term to be added to the friction factor which incorporated unsteady flow conditions, however the inclusion of an iterative method of calculating friction causes calculation times to increase and leads to serious 'overshoot' at early time steps in the calculation[5].

$$\Delta P = \frac{4f\rho LV^2}{2D} + \frac{16\rho L}{D^2}\sum \begin{bmatrix} V(time - j\Delta t + \Delta t) \\ -V(time - j\Delta t - \Delta t) \end{bmatrix} W(t^*(j\Delta t)) \qquad \textbf{Eq. 1}$$

Zilke's research of unsteady friction in laminar flows produced the basis for the prediction of the rate of change. The unsteady frictional pressure loss in pipe flow is calculated using

$$\Delta P = \frac{4f\rho LV^2}{2D} + \frac{16\rho L}{D^2}\int_0^1 \frac{\partial V}{\partial t^*} W_o(t - t^*)dt^* \qquad \textbf{Eq. 2}$$

Where t^* is non-dimensional time

$$t^* = \frac{4vt}{D^2} \quad \textbf{Eq. 3}$$

Vitkovsky *et al*[12] extends Zilke's work, presenting an equation which is applicable to turbulent flows.

$$\Delta P = \frac{4f\rho LV^2}{2D} + \frac{16\rho L}{D^2}\sum_{1,3,5}^{M}\begin{bmatrix}V(time - j\Delta t + \Delta t)\\ -V(time - j\Delta t - \Delta t)\end{bmatrix} W\left(t^*(j\Delta t)\right) \quad \textbf{Eq. 4}$$

Frictional loss defined as:

$$\Delta P = \frac{4f\rho LV^2}{2D} \quad \textbf{Eq. 5}$$

The Colebrook-white relationship was developed in 1939 is based on an earlier body of research by C.F. Colebrook and C.M. White '*Experiments with fluid friction in roughened pipes'*. Colebrook's 1939 publication *'Turbulent flows in pipes with particular reference to the transition region between smooth and rough pipes laws'* set out the following equation which is still used today for the calculation of the friction factor in turbulent air flow in pipes.

$$\frac{1}{\sqrt{f}} = -4log_{10}\left(\frac{\varepsilon/D_h}{3.7} + \frac{1.26}{Re\sqrt{f}}\right) \quad \textbf{Eq. 6}$$

Where, f is the friction factor, ε is the roughness (m), D_h is the hydraulic diameter or internal diameter of a pipe, Re is the Reynolds number.

$$Re = \frac{\rho VL}{\mu} = \frac{VL}{\mu_k} \qquad \text{Eq. 7}$$

Where, V is the mean velocity of the flow in the pipe (m/s), L is the pipe length, μ is the dynamic viscosity of the fluid, μ_k is the kinematic viscosity and ρ is the density of the fluid.

2.1 Existing building drainage system modelling techniques

2.1.1 Method of Characteristics and AIRNET

Since its development as a usable modelling tool in the 1960s, the MoC has been extensively used for solving the Saint Venant equations (a 1D simplification form of the fully developed Navier Stokes equations) to describe the laws of continuity and momentum in shallow water flow problems. This technique based on characteristic lines along which the governing equations are transformed (from partial differential equations to become ordinary differential equations), provides the advantage of rapid computation of supersonic flows within simple geometries.

Figure 1, Typical grid representative of the scheme used for the calculation of the propagation of pressure transients through a pipe.

This technique is rooted on the principle that the supersonic flow is hyperbolic, meaning that a given point has effect on some region downstream of it, but not upstream[14]. The characteristic lines which emanate from or intersect at a given point, describe the two boundaries of the region in reference. The calculation at a certain time on the grid is based on the conditions upstream and downstream, as one step in the past, and requires a definition of the characteristic slope as a foundation for all future predictions.

In actuality, these lines should be curved, however as the time steps are normally very small, and so representing this data in straight lines introduces little error to the calculation. Information regarding air velocity and wave speed and hence pressure, is calculated and transferred through these lines of communication formed by the characteristic slopes allows to be propagated throughout the system[12].

AIRNET, is a MoC based finite difference (FD) model which was developed at Heriot-Watt University initially by the late Professor Swaffield[5] and is under continued development. This model simulates real system boundaries and appliance trap seals within a building drainage vent system.

2.2 Boundary conditions

The MoC solution technique divides the BDS up into its constituent parts. Therefore creating what can be considered a listing of domains each with inlet and outlet otherwise written as C^+ characteristic (at a downstream boundary) and C^- characteristic (at the upstream boundary). A single equation is used to describe the effect of the domain's characteristic on the flow regime. This equation is known as the boundary equation.

Figure 2, Boundary conditions and characteristic curves for a typical single stack building drainage system

Boundary condition development approaches

The MoC techniques described, requires the initial conditions to be known so that the process of numerical modelling can begin. These nodes are solved by first developing boundary conditions which are compatible with a single C^+ and C^- characteristic. For every entry to and exit from a pipe section one characteristic exists.

Existing water trap seal boundary conditions

The boundary condition for the water trap seal represents water movement in response to air pressure forces from the system side, abated by friction and separation losses. This device, connected to a network is immediately vulnerable as it is responsive to positive and negative pressure transients, causing fluctuations in water level (much like in a manometer).

The existing water trap boundary condition in AIRNET consists of 4 terms such that;

$$T1 + T2 - T3 - T4 = 0 \qquad \textbf{Eq. 8}$$

Frictional resistance for trap seal oscillation is represented in the T3 term., where;

$$T3 = \tau LP = 0.5 \rho f L P V_{trap}^2 \qquad \textbf{Eq. 9}$$

The V^2 term refers to water in the trap and it is this term that will be manipulated to represent the response to air pressure transients of different frequencies.

For completeness the other terms are shown below.

$$T1 = A\left[0.5\left(P_{pipe,t+\Delta t} + P_{pipe,t}\right) - \left(P_{atm} + P_{room}\right)\right] \qquad \textbf{Eq. 10}$$

$$T2 = \rho g A(H_o - H_1 + 2dH) \quad \textbf{Eq. 11}$$

$$T4 = \rho L A \frac{V_{trap,t+\Delta t} - V_{trap,t}}{\Delta t} \quad \textbf{Eq. 12}$$

Where Eq. 10 is the pressure differential between the room air and the transient pressure profile in time, Eq. 11 is the height differential between the water surface on the system and appliance side of the curved conduit, Eq. 9 is the frictional resistance to the movement of water in the trap or trap oscillation, and Eq. 12 is the mass acceleration.

3 Methodology

The methodology employed was to model the water trap seal in ANSYS CFX and then to analyse the flow characteristics in order to derive a more comprehensive boundary condition suitable for application in AIRNET.ANSYS CFX is a general purpose computational fluid dynamics software which uses a hybrid discretisation method for the solution of partial differential equations. This hybrid “element based FVM” requires the generation of an unstructured grid where elements, nodes and control volumes are determined. ANSYS CFX is an Implicit solver meaning that no limitation exist on its time step size.

The CFD simulation must progress through three stages: pre-processor, solver, post processor.

3.1 Definition of appliance geometric parameters

The two appliance water traps modelled can be described as: the glass appliance part swivel water trap by Schott, and a typical PVC (commercially available)

appliance water 'P' trap. They are henceforth referred to within this text as the laboratory and commercial appliance water traps respectively. The geometric differences between the two reference water traps is noted in the size of the inner bend (12.5mm, 37.5mm), the internal diameter of the conduit (46mm, 40mm), the overall height of the trap (212mm, 172mm), and the overall shape of the trap (P shaped, swivel) for the commercial and laboratory traps respectively.

The CFD problem was described to be transient in nature, with the end of calculations occurring after 0.5 (simulation) seconds.

Figure 3, Side view of the laboratory appliance trap digitally reproduced using ANSYS design modeller showing specified entry and exit boundary conditions.

Figure 4, Front view of the commercial water trap digitally reproduced using ANSYS design modeller, showing specified entry and exit boundary conditions.

3.2 Computational mesh

The finite positions for observation and data collection impose no disruption to the flow regime, therefore the accuracy of the data is largely dependent on the computational specification. The geometry of the commercial trap was meshed with tetrahedral cells and the laboratory trap was meshed with prisms and hexahedrons.

Figure 5, The computational mesh applied to the commercial appliance water trap

A no-slip wall boundary was applied at the pipe wall.

A single domain was created within which the inlet, outlet and body of the trap were defined. The mesh generated is derived of 806,215 elements, 832,128 nodes, 52,468 faces, and constructed predominantly from the 804,683 hexahedrons but also by the addition of 1,532 prisms. The commercial trap mesh generated (see Figure 5) is derived of 4,541 elements, 20,528 nodes, 4116 faces, and constructed predominantly from the 20,528 tetrahedrons. The comparable fine mesh in the commercial trap model, is derived of 4,424,807 elements, and 889,592 nodes.

3.3 Appliance water trap boundary conditions

In typical building drainage systems, water and air are the main fluids, accompanied intermittently by traces of: detergent, bodily waste and food waste. For the purpose of this research, only water and air are considered.

In order to clearly define the free surface region, an expression was defined and written in ANSYS CFX expression language (CEL). The free surface boundary was after several experimental methods defined by:

$$VF_{air} = if(y\ coordinate > (H - H_s - D - W_T)[m],\ 1,\ 0) \qquad \textbf{Eq. 12}$$

Where, W_T is the pipe wall thickness, D is the uniform diameter of the trap, H is the total height of the trap, H_s is the seal height.

and the volume fraction of water as,

$$VF_{water} = 1 - VF_{air} \qquad \textbf{Eq. 13}$$

The volume fraction (VF) of air and water is calculated per cell in the domain. For instance, an average scale shows that with a 38mm trap seal in the traditional water trap the average initial VF of air is 0.62459 and water, 0.3754. Meaning that at t = 0, 62.5% of the trap is filled with air and 37.5% is filled with water, thus creating the air and water columns. Volume fractions are always written as a ratio of the phases and sum to 1.

The boundaries at the pipe inlet (system side) and pipe outlet (appliance side) were pressure specified, and a fully developed sinusoidal altering pressure gradient, and a zero static pressure with atmospheric conditions specified respectively. Five (5) simulations were conducted for each appliance water trap. With each simulation the frequency of the applied pressure varied while the maximum amplitude of the pressure wave remained constant.

$$Sine\ wave\ input = 100[pa] \times sin(2\pi fT) \qquad \textbf{Eq. 14}$$

Where T (current time), is divided by 1[s] to create a dimensionless figure.

3.4 Angled data planes analysis method

In order to determine a relationship between the water column movement along the bend in the general direction of flow and velocity, a 'slice plane approach was used (see Figure 6). Seven planes were selected at 30º increments from the centre of the bend, and named starting from the right: 0 º, 30 º, 60 º, 90 º, 120 º, 150 º and 180º.

All data was collected at the first positive peak along the sinusoidal cycle to enable comparison based on equivalent applied pressure amplitude to be made.

Figure 6 presents the position of the data points along the slice planes in the commercial and laboratory appliance water traps, the XY and ZY coordinates for the laboratory and commercial traps respectively, along with the position of the water line at time equals zero is shown.

Figure 6, Geometric representation of the appliance trap seals (a) laboratory trap, (b) Commercial trap seal - 30º increment monitor planes and selected data points (inner, middle & outer points)

3.4.1 Turbulence model

The Shear Stress Transport model used in the prediction of the air and water column movement in the water trap, is a variation of Menter's model; developed to combine the standard $k\varepsilon$ model with the standard $k-\omega$ model in order that the inner region of the boundary layer be adequately resolved by the latter, while the former is employed to obtain solutions in the outer part of the boundary layer[15]. A blending function is used to provide a smooth transition between the two models.

4 Results and discussion

Figure 7 shows the general form of fluid flow across all frequencies and traps tested at varying angled planes across the water trap seal; observing flow only along the inner, middle and outer sections on the planes.

The movement zones are:

Zone 1	0º to 30º	acceleration in the velocity profile (damping zone)
Zone 2	30 º to 150º	largest velocity gradient but velocity across planes remain constant

Zone 3 150º to 180º deceleration in the velocity profile (damping zone)

Figures 6 to 9 illustrate the identified zones of movement. Zone 1 and 3 represent the entrance and exit of the water seal bend respectively, display the greatest resistance to movement, while water zone 2 is found to propagate at a constant rate.

Figure 7, The average velocity along the inner, middle and outer bend of both appliance trap seals at various angles (clockwise) from the centre of the pipe bend along all frequencies.

4.1.1 Frequency analysis

Gormley and Beattie[16] hypothesised a direct correlation between frequency of applied pressure wave and frictional losses in the curved U-bend. A frequency analysis of the CFD outputs was carried out to enhance and validate this previous work.

Figure 8 (a) the laboratory trap seal and (b) the commercial trap seal, shows the velocity variance across the water trap seals. Velocity data across the slice planes noted in Figure 6 is plotted against the distance from the innermost point. Comparison is proposed between the results when the transient air pressure is 1Hz verses 8Hz.

In the laboratory trap seal bend – at low frequencies the acceleration of the flow regime occurs in the first segment (0-30 degrees) along both the inner and the outer surfaces and the sixth segment (150 – 180 degrees) along the outer surface, while the velocity of the flow in the middle of the conduit it found to be greater than that at the inner bend (see Figure 8, 1Hz (a)). The greatest displacement of the water is found at 1Hz, a finding supported by Gormley and Beattie[16] and Swaffield[5] .

The zones of movement identified in Figure 9 remain applicable in Figure 8 (a) 1Hz, 3Hz and 8 HZ of the laboratory appliance trap seal. Here, in the first segment of observed movement, acceleration is recorded at all monitored points with the greatest increase noted along the inner surface of the bend. As in Figure 8, 1Hz (a) the movement along the 30^o,60^o,90^o,120^o and 150^o lines of the curved conduit remain steady along the inner, middle and outer data points. **Figure 8, The velocity along the inner, middle and outer bend of (a) Laboratory trap seal, and (b) Commercial trap seal at various angles (clockwise) from the centre of the pipe bend when input pressure is 1, 3 & 8 Hz**

Figure 8 (b) presents the likely flow pattern along the curve of the water seal for frequencies 1Hz, 3Hz and 8Hz in the commercial trap. This flow regime provides an exception to the general zones of movement identified in Figure 9, as here the acceleration along the inner bend is not stopped at 30º, but rather at 60 º. This exception does not hold for the middle and outer bend velocities as they remain as earlier predicted; transitioning at 30º. Figure 9 presents a revised pictorial representation of the zonal regions within the commercial appliance water trap.

Figure 9, Representation of the zones of movement in the commercial appliance trap seal

An additional shared feature between the flow patterns along the two traps is that at 180º (the end of zone 3) all trends tend towards each other; providing a reduced differential. This convergence of velocity ranges is a significant observation as it suggests reduced movement of the water. Note that data shown in Figure 10 (Zone 3a and 3b) at 1 hz has a velocity differential of 0.0247m/s and 0.07399 m/s and at 8 hz, has a velocity differential of 0.00524m/s and 0.013248m/s across the 180° slice plane. In reality this means that the velocity profile changes with frequency and the differential in velocity across the trap diameter causing inconsistent movement. At lower frequencies this sets up an oscillation of water movement leading to much

greater movement. This, in effect, is what the existing AIRNET boundary condition cannot predict.

Figure 10, Velocity along Zone 1, 2 and 3 for all applied pressure frequencies in the laboratory appliance trap (a) and the commercial appliance trap (b). Distance along the x plane is a measure from the intersection of plane with the inner bend.

Figure 10 presents the velocity along the slice planes at 0º (Zone 1), the beginning of Zone 2 and the end of Zone 3 in the laboratory trap seal (a) and the commercial trap seal (b) for all frequencies. It can be concluded that for the same applied pressure the rise time is critical to the speed at which the water column is moved in response.

4.2 Comparison of the two traps

Comparisons between the behaviour of the water column in the two modelled appliance water traps have been made in the previous section. It has been shown that:

1. The water velocity along the trap with the smaller inner length is consistently greater than that in the trap with the larger inner circumference regardless of the applied frequency. Note the y axis values of Figure 10.
2. The rise time (and therefore wave frequency) of the low amplitude pressure transient plays a critical role in the recorded water velocity. Figure 10 shows that regardless of the zone, the water velocity recorded is closely linked the applied air pressure transient frequency.
3. The inner length of Zone 1 is the only length comparable between two differing U-bend trap seals. This being as zone 1 in the Commercial trap seal is altered to reflect the data. This alteration makes the inner zone length comparable to the inner zone length of the Laboratory trap seal
4. The greater the applied frequency of the applied transient, the lower the variance between the velocity across the planes
5. At low frequencies the flow in the Laboratory trap becomes increasingly unsteady unlike in the Commercial trap where the general flow trends remain consistent.

By considering the velocity gradients across the planes set at 30° increments it was found that the velocity differential across the trap is greater in the trap with the smaller diameter and also that a general change in flow occurs between 2 and 4 hz.

The data showed the anomaly that is the flow behaviour along the 0º plane of the laboratory trap. The water level in this trap lies 2mm above this plane at time equal to zero. At 0.25s in the 1Hz simulation, the water level is below this original point. The recorded water volume fractions along this plane are: 0.00000185 (inner), 0.0000031 (middle) and 0.00218(outer). At low frequencies there is greater movement of water and this 0 º plane or rather this seemingly free surface plane, would be the first to approach a water volume fraction less than 1.

As the diameters of the traps differ by 6mm, the following equation was employed to present a platform for comparison at various points along the planes.

$$t = \frac{d}{D} \qquad \textbf{Eq. 15}$$

Where, d is the distance from the inner surface, and D is the internal diameter of the trap.

In the commercial trap seal the average velocity relationship across the surface after bend at x=0 (middle point) is described as follows,

$$\frac{\sum_{i=0}^{n} V_{mf}}{n} = \frac{\sum_{i=0}^{n} 0.0857e^{-1.234i}}{n}, \quad i \in [0,1] \qquad \textbf{Eq. 16}$$

In the laboratory trap seal equation the mean velocity is

$$\frac{\sum_{i=0}^{n} V_{mf}}{n} = \frac{\sum_{i=0}^{n} 0.0235i + 0.0496}{n}, \quad i \in [0,1] \qquad \textbf{Eq. 17}$$

Where, n is the number of points along the plane selected.

The examination of the proportional relationship between the velocities along the inner, middle and outer bend of the two traps, and reiterated that not only does the movement of water become consistent at velocities greater than 3Hz, but suggests the relationship between this movement in traps (of differing geometric characteristics), is constant between 3Hz and 8Hz. As stated previously, two distinct regions exist: below and above 3Hz. Henceforth, the transitional region will be considered to occur between 3 and 4 Hz.

This circumference of the inner bend was calculated to be:

- 45.6 mm in the commercial trap
- 113.1 mm in the laboratory trap

The ratio of the inner bend length (L_i) and the outer bend length (L_o) in the commercial trap and laboratory trap is 0.242 and 0.473 respectively.

To derive a suitable coefficient linking inner and outer bend length and velocity;

Let

$$v_L = v * \frac{L_I}{L_O} \qquad \textbf{Eq. 18}$$

Where, v is the velocity at the data point, and $\frac{L_I}{L_O}$ is the ratio between the inner and outer bend circumference.

and

$$V_L - \frac{\sum_{i=0}^{n}(v * \frac{L_I}{L_O})}{n} \quad \text{Eq. 19}$$

This data was determined by taking the average velocity across all data points for each frequency then multiplying it by the L_I/L_O ratio. The following relationships were found:

$$V_L = 0.1253 t_{fpp} \quad \text{Eq. 20}$$

Where, V_L is the mean velocity as a function of the bend length ratio, and t_{fpp} is time at first positive peak. It follows that:

$$t_{fpp} = \frac{1}{4f} \quad \text{Eq. 21}$$

The following equations serve as a general description for velocity in the laboratory or commercial appliance water trap, and enable prediction of water seal flow rate dependent on trap geometry. They are written in the form $(S_v i + c_L)\frac{L_O}{L_I}$.

$$v = \left((-0.0888 t_{fpp} + 0.00002)i + 0.1645 t_{fpp}\right)\frac{L_O}{L_I}, \quad if\ \theta \in [0º] \quad \text{Eq. 22}$$

$$v = \left(\left(-0.1105t_{fpp} - 0.002\right)i + 0.2062t_{fpp}\right)\frac{L_o}{L_I}, if\ \theta \in [30º, 150º] \quad \textbf{Eq. 23}$$

$$v = \left(\left(-0.0434t_{fpp} - 0.0032\right)i + 0.1647t_{fpp}\right)\frac{L_o}{L_I}, if\ \theta \in [180º] \quad \textbf{Eq. 24}$$

Figures 11 and 12 show the results of the CFD analysis (measured) plotted against the results of Eq 22, Eq.23 and Eq. 24.

Figure 11, **Measured (CFD) vs predicted velocity along the Laboratory trap seal at 2Hz (time: 0.125s) $R^2 = 0.9163$**

Figure 12, **Measured (CFD) vs predicted velocity along the Commercial trap seal at 2Hz (time: 0.125s). $R^2 = 0.8948$**

Figure 13, Methodology flowchart for boundary condition development of the water trap seal.

The zones of movement within the appliance trap seals are comparable as they occurred between 15-18mm of the beginning of the bend, then until the 150 degree plane, and from the 150 to 180 degree plane; correlating to zones 1, 2 and 3 respectively. It was discussed previously that friction is a measure of an object or fluid's resistance to motion. Zone 1 and Zone 3 portray exactly this as the velocities recorded in these zones were always less than the velocity in Zone 2. Friction therefore can be said to be a measure of the differential between the zones of movement.

The relationships between the maximum recorded velocity along the inner bend (which occurs within zone 2) and the velocities in zone 1 and 3 was further

investigated. The following relationship was developed and used in AIRNET as a boundary condition which reflects the unsteady friction occurring in water trap seals.

$$\Delta v_i = 0.0478 t_{fps} + 0.0002 \qquad \text{Eq. 25}$$

4.3 Frequency response

Gormley and Beattie[16] identified the transitional zone of movement through laboratory investigation of the response of water trap seal to a number of pressure frequencies. This zone is confirmed by the CFD simulations of the laboratory of like geometric proportions. Here the analysis of the results found that a transitional zone of a significant altering of trap velocity is between 3 and 4 Hz.

Figure 14, Observation of the displacement of water in the appliance trap in the Heriot- Watt University drainage laboratory.

Figures 14 and 15, show the disproportional displacement of water along the bend as air displaces the water. This is a result of a positive pressure transient in the laboratory and CFD investigation when an air pressure of significant amplitude and/or frequency is applied.

The pattern of movement in the laboratory trap validates the flow regime in the CFD model. However when the photographs are overlaid a discrepancy is noted to the right of the outer bend. This area in highlighted in Figure 16.

Figure 15, Air volume fraction across the XY plane (Z=0) in the laboratory appliance water trap at 0.5s when an applied 1Hz pressure transient.

Figure 16, The overlay of the laboratory observation image and the VF results of the appliance trap seal from ANSYS CFX

Gormley and Beattie[16], investigated a single trap seal's water movement. Using a high speed camera, this work captured the trap seal movement along the appliance side of the trap. Figure 17 presents the comparable images above the base line height and for frequencies, 1,2,3,4 and 8 for the 38mm trap seal test.

Figure 17, Representative sketches of the water oscillations for each tested frequency (a) Measured at 38mm water trap depth, adapted from Gormley and Beattie[16], (b) Predicted using ANSYS CFX at 38mm water trap depth

The pattern of water movement along the appliance side of the water trap seal is found to be similar to that calculated by ANSYS CFX. This data was gathered through visual assessment. Comparisons are therefore deemed to be valid.

5 Validation of Frequency dependant representation of velocity change

AIRNET predictions of water trap responses for a pressure input to the branch of 1 metre length, connected to the likened virtual model of the laboratory trap, are shown below. Two cases were simulated

i) Using the existing boundary equation, a single peak pressure was applied the virtual water trap seal at frequencies of 1, 3, 5, 8, and 10Hz.

ii) The friction factor developed in this study using the average velocity across zone 2 (in the water trap) as it covers a wider area of movement than zones 1 and 3. Delta v here is a function of L for the two modelled appliance trap seals.

The following presents the results of the water seal movement in the virtually tested appliance trap seal using the delta v friction factor (equation 25).

Figure 18, Comparison of water trap seal movement from predictions based on the existing boundary condition, the new delta *v* boundary condition and measured data from Gormley and Beattie[16]

Generally, the existing boundary condition overestimates the trap seal movement which leads to an overestimation of seal loss. It follows that this overestimation suggests an inaccurate whole system assessment of the system's operational characteristics. The new boundary condition is frequency dependent, providing more realistic estimation of effects of air pressure transient propagation, trap water movement and therefore trap seal loss. Figure 18 also shows the movement observed by Gormley and Beattie[16]. It can clearly be seen that the new new delta v boundary condition closely correlates with the measured data.

6 Conclusions

This research has produced a new method for evaluating performance and generating dynamic boundary conditions suitable for inclusion in the existing 1-D MoC based model, AIRNET; which solves for pressure and velocity via the St. Venant equations of continuity and momentum in a finite difference scheme.

The key findings from this research can be summarised as follows;

- The protection afforded by trap seals of all types is dependent on the frequency of the applied pressure wave as well as the amplitude of force applied.
- Current models can overestimate water trap movement (and hence water loss) at higher frequencies (> 3Hz)
- The use of CFD to evaluate water trap seal movement and for the development of boundary expressions suitable for inclusion in a MoC model has proved effective.
- Identification of the transitional frequency region comparable to previous empirical research along with the visual observations of the pattern of flow movement suggests that this technique is a suitable alternative to laboratory testing.
- A dynamic velocity decrement model encapsulating unsteady friction and separation losses linked to device geometry has been developed for the first time.
- Analysis of velocity profiles at different locations suggest that water trap seals with a smaller inner bend length are more vulnerable to induced siphonage.

Improved methods of boundary condition development for the 1-D MoC model using CFD output data confirms the link between frequency of applied pressure wave and water level response, indicating that a more robust friction model is required for such complex turbulent flow situations.

References

1. WHO (2003a) Consensus document on the epidemiology of severe acute respiratory syndrome (SARS). Department of Communicable Disease Surveillance and Response, World Health Organisation,

2. WHO (2003b) Inadequate plumbing systems likely contributed to SARS transmission, Press Release WHO/780,26 September, World Health Organisation, Geneca, pp.1-2.

3. Hung HCK, Chan DWT, Law LKC, Chan EHW and Wong ESW. Industrial experience and research into the causes of SARS virus transmission in a high-rise residential housing estate in Hong Kong, *Building Services Engineering Research and Technology*,2006; **27**(2): 91—102.

4. Gormley, M., Swaffield, J., Sleigh, P. and Noakes, C. (2011). An assessment of, and response to, potential cross-contamination routes due to defective appliance water trap seals in building drainage systems. *Building Services Engineering Research and Technology,* 33(2), pp.203-222.

5. Swaffield, J. (2010). *Transient airflow in building drainage systems*. Abingdon, Oxon: Spon Press.

6. Bennett, J. and Brachman, P. (1998). *Hospital infections*. Philadelphia: Lippincott-Raven.

7. Hathway, E., Noakes, C., Sleigh, P. and Fletcher, L. (2011). CFD simulation of airborne pathogen transport due to human activities. *Building and Environment*, 46(12), pp.2500-2511.

8. Gormley M, Aspray TJ, Kelly DA, Rodriguez-Gil C (2017) Pathogen cross-transmission via building sanitary plumbing systems in a full scale pilot test-rig. PLoS ONE 12(2): e0171556. doi:10.1371/journal.pone.0171556

9. Carstens, M. and Roller, J. (1959). Boundary-shear stress in unsteady turbulent pipe flow. *Journal of the Hydraulic Division, ASCE*, 65(HY2), pp.67-81.

10. Zilke W. (1968). Frequency dependant friction in transient pipe flow, *Journal of Basic Engineering*. Trans. ASME, Vol 90, No. 1, pp.109-115.

11. Vitkovsky, J.P., Stephens, M.L., Bergant, A., Simpson, A.R., &Lambert, M.F.(2004) Efficient and accurate calculation of Vardy-Brown unsteady friction in pipe transients. 9th International Conferenec on Pressure Surges, Chester, U.K. 24-26 March.

12. Swaffield, J. and Boldy, A. (1993). *Pressure surge in pipe and duct systems*. Aldershot, Hants, England: Ashgate Pub.

13. Murzionak, A. (2013). *Rocket Based Combined Cycle Exchange Inlet Performance Estimation at Supersonic Speeds*. MSc Thesis. Carleton University, Ontario, Canada.

14. Douglas, J., Gasiorek, J., Swaffield, J. and Jack L. (2011). *Fluid mechanics*. Harlow, Essex, England: Longman Scientific & Technical.

15. Yeoh, G.H. and Tu, J.Y. (2009) Computational techniques for multiphase flows: Basics and Applications. Butterworth-Heinemann, Elsevier, U.K.

16. Gormley M. and Beattie R.K. (2010) 'Derivation of an empirical frequency dependent friction factor for transient response analysis of water trap seals in building drainage systems' *(2010) Building Services Engineering Research & Technology 31,3 pp. 221-236.*

Figures captions

Figure 1, Typical grid representative of the scheme used for the calculation of the propagation of pressure transients through a pipe.

Figure 2, Boundary conditions and characteristic curves for a typical single stack building drainage system

Figure 3, Side view of the laboratory appliance trap digitally reproduced using ANSYS design modeller showing specified entry and exit boundary conditions.

Figure 4, Front view of the commercial water trap digitally reproduced using ANSYS design modeller, showing specified entry and exit boundary conditions.

Figure 5, The computational mesh applied to the commercial appliance water trap

Figure 6, Geometric representation of the appliance trap seals (a) laboratory trap, (b) Commercial trap seal - 30º increment monitor planes and selected data points (inner, middle & outer points)

Figure 7, The average velocity along the inner, middle and outer bend of both appliance trap seals at various angles (clockwise) from the centre of the pipe bend along all frequencies.

Figure 8, The velocity along the inner, middle and outer bend of (a) Laboratory trap seal, and (b) Commercial trap seal at various angles (clockwise) from the centre of the pipe bend when input pressure is 1, 3 & 8 Hz

Figure 9, Representation of the zones of movement in the commercial appliance trap seal

Figure 10, Velocity along Zone 1, 2 and 3 for all applied pressure frequencies in the laboratory appliance trap (a) and the commercial appliance trap (b). Distance along the x plane is a measure from the intersection of plane with the inner bend.

Figure 11, Measured (CFD) vs predicted velocity along the Laboratory trap seal at 2Hz (time: 0.125s) $R^2 = 0.9163$

Figure 12, Measured (CFD) vs predicted velocity along the Commercial trap seal at 2Hz (time: 0.125s). $R^2 = 0.8948$

Figure 13, Methodology flowchart for boundary condition development of the water trap seal.

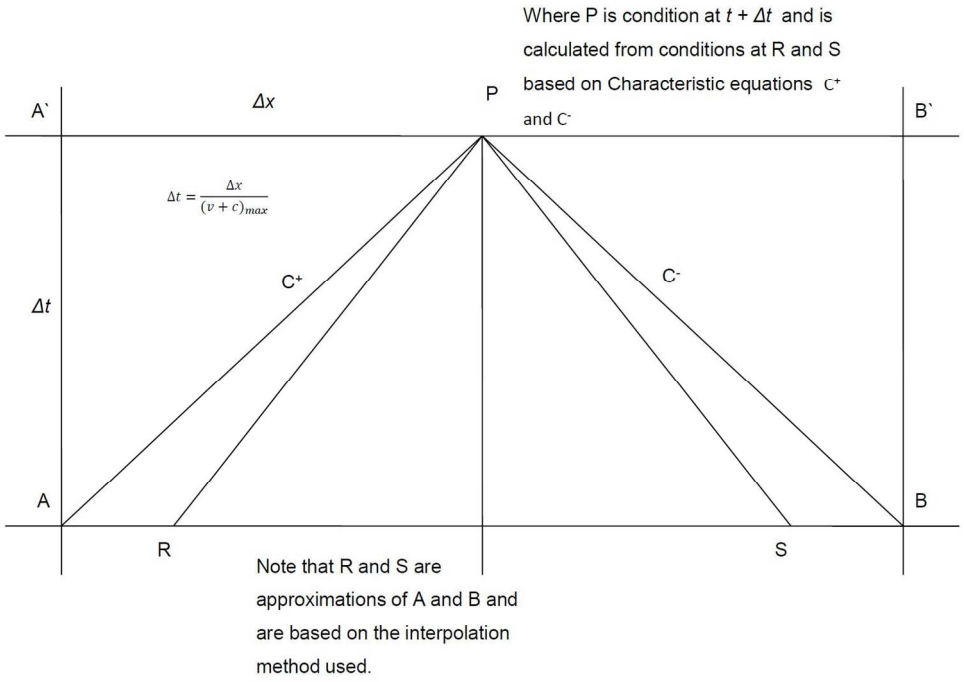

Figure 1, Typical grid representative of the scheme used for the calculation of the propagation of pressure transients through a pipe.

232x163mm (192 x 192 DPI)

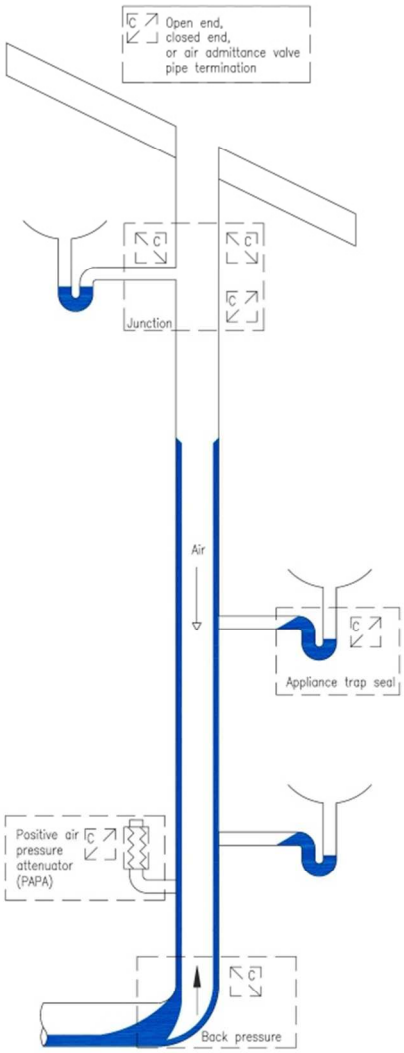

Figure 2, Boundary conditions and characteristic curves for a typical single stack building drainage system

191x270mm (96 x 96 DPI)

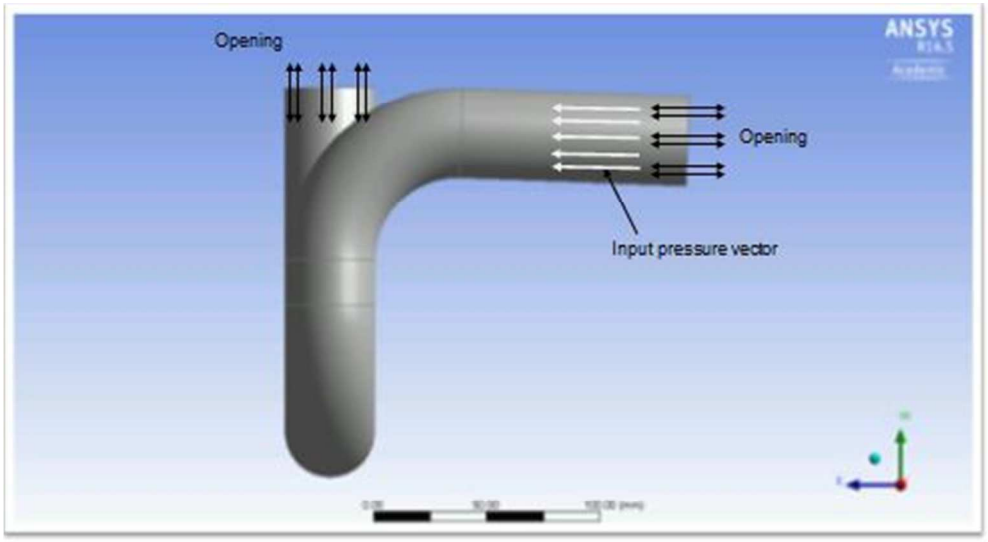

Figure 3

Figure 3, Side view of the laboratory appliance trap digitally reproduced using ANSYS design modeller showing specified entry and exit boundary conditions.

130x78mm (96 x 96 DPI)

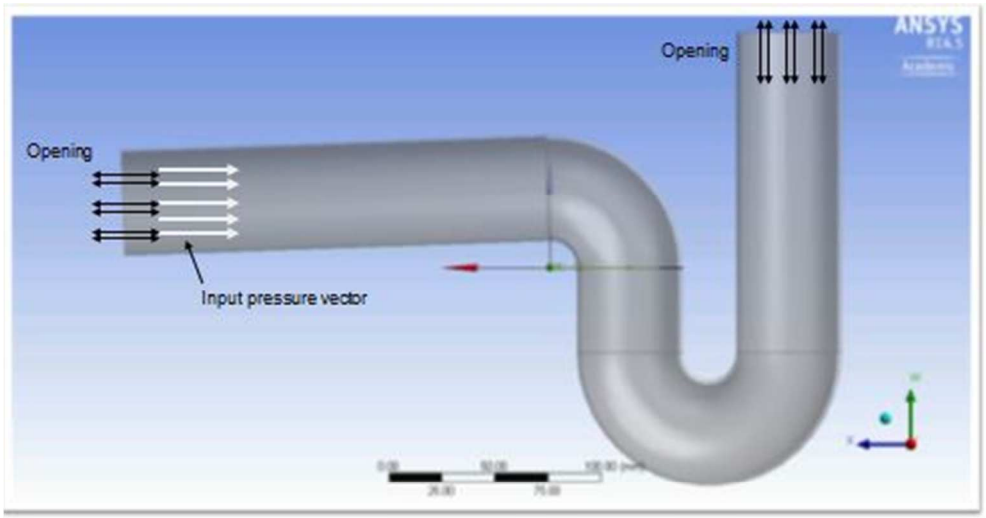

Figure 4,

Figure 4, Front view of the commercial water trap digitally reproduced using ANSYS design modeller, showing specified entry and exit boundary conditions.

130x75mm (96 x 96 DPI)

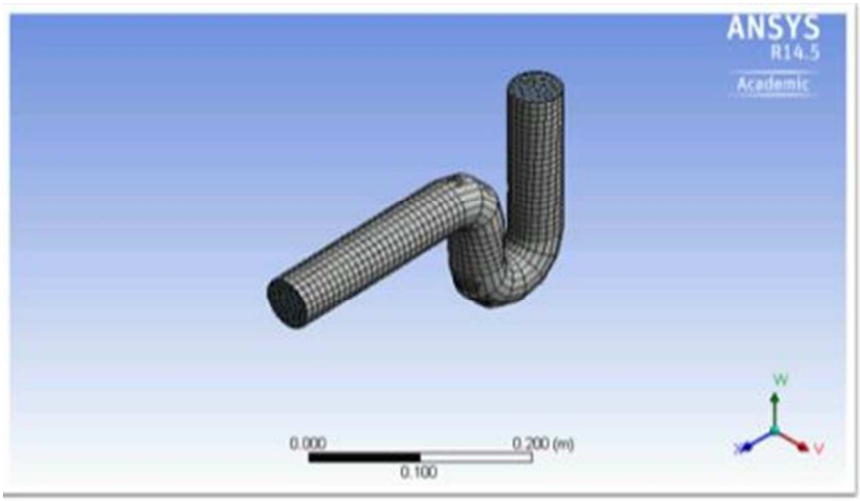

Figure 5

Figure 5, The computational mesh applied to the commercial appliance water trap

123x78mm (96 x 96 DPI)

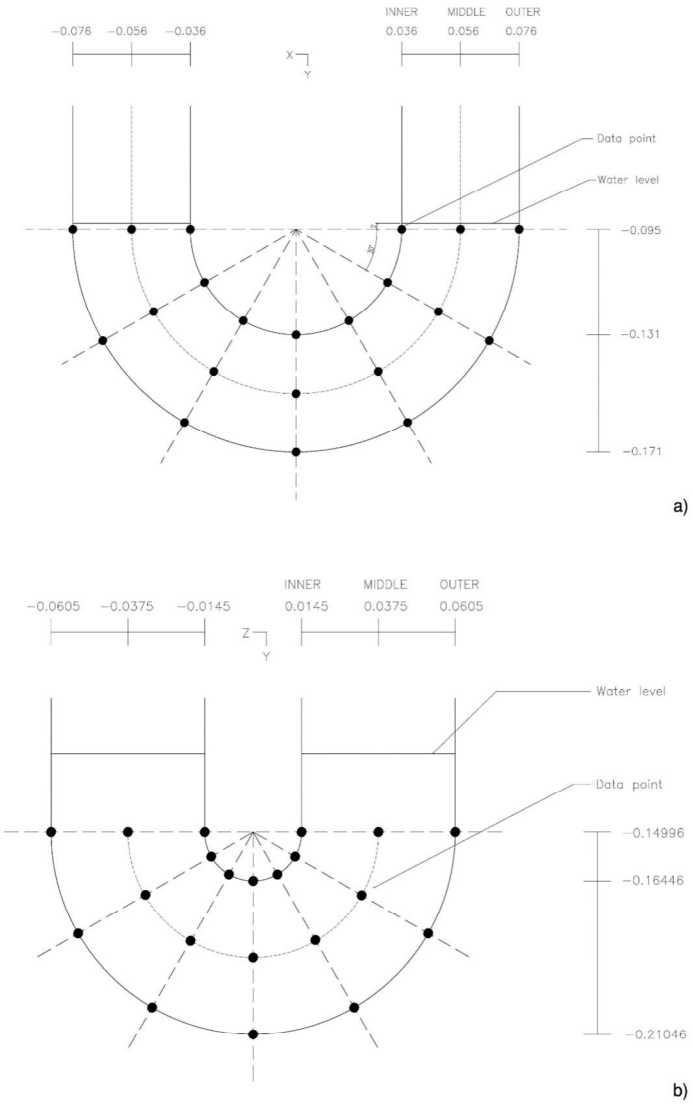

Figure 6, Geometric representation of the appliance trap seals (a) laboratory trap, (b) Commercial trap seal - 30º increment monitor planes and selected data points (inner, middle & outer points)

170x244mm (192 x 192 DPI)

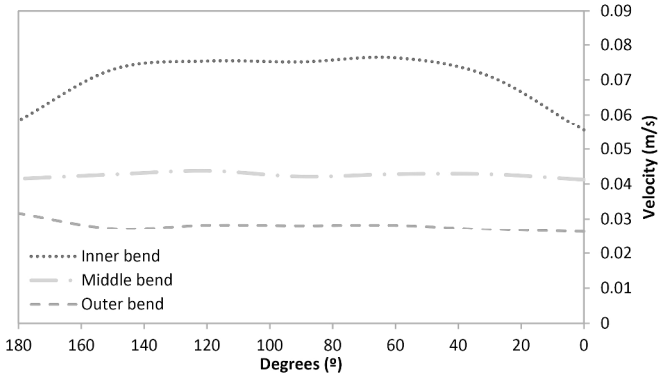

Figure 7, The average velocity along the inner, middle and outer bend of both appliance trap seals at various angles (clockwise) from the centre of the pipe bend along all frequencies.

297x344mm (300 x 300 DPI)

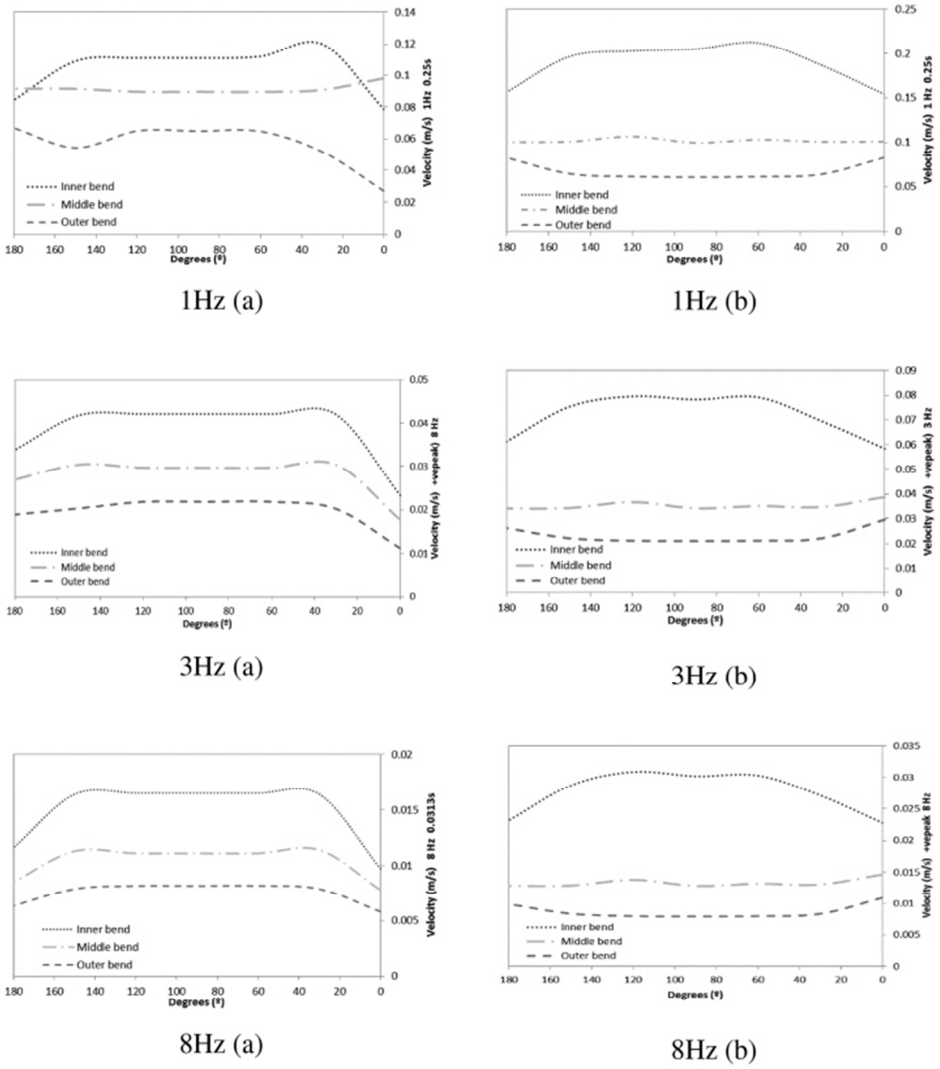

Figure 8, The velocity along the inner, middle and outer bend of (a) Laboratory trap seal, and (b) Commercial trap seal at various angles (clockwise) from the centre of the pipe bend when input pressure is 1, 3 & 8 Hz

203x235mm (96 x 96 DPI)

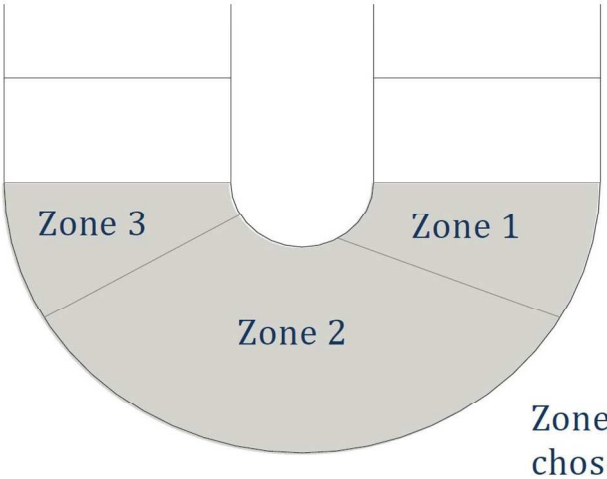

Zones 1,2 and 3 chosen to analyse water velocity profiles at entry, bend and exit of trap.

Figure 9, Representation of the zones of movement in the commercial appliance trap seal

203x154mm (192 x 192 DPI)

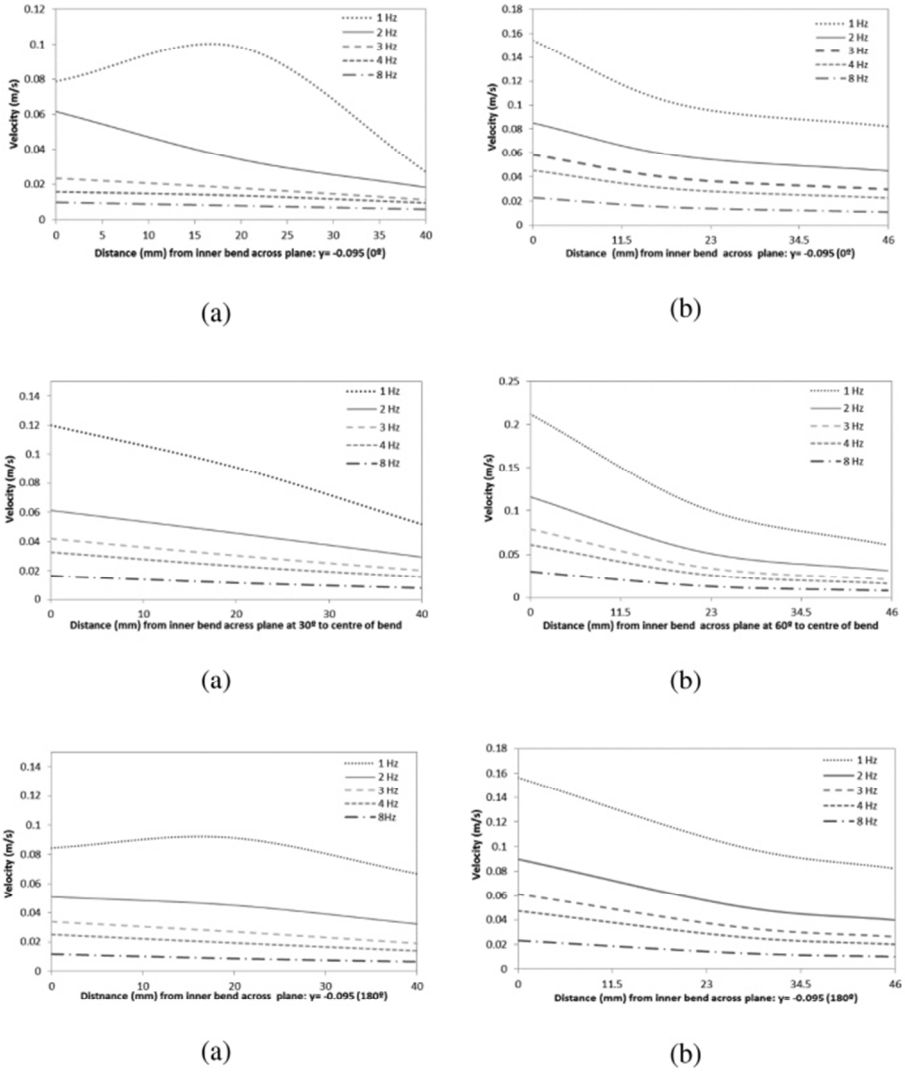

Figure 10, Velocity along Zone 1, 2 and 3 for all applied pressure frequencies in the laboratory appliance trap (a) and the commercial appliance trap (b). Distance along the x plane is a measure from the intersection of plane with the inner bend.

203x235mm (96 x 96 DPI)

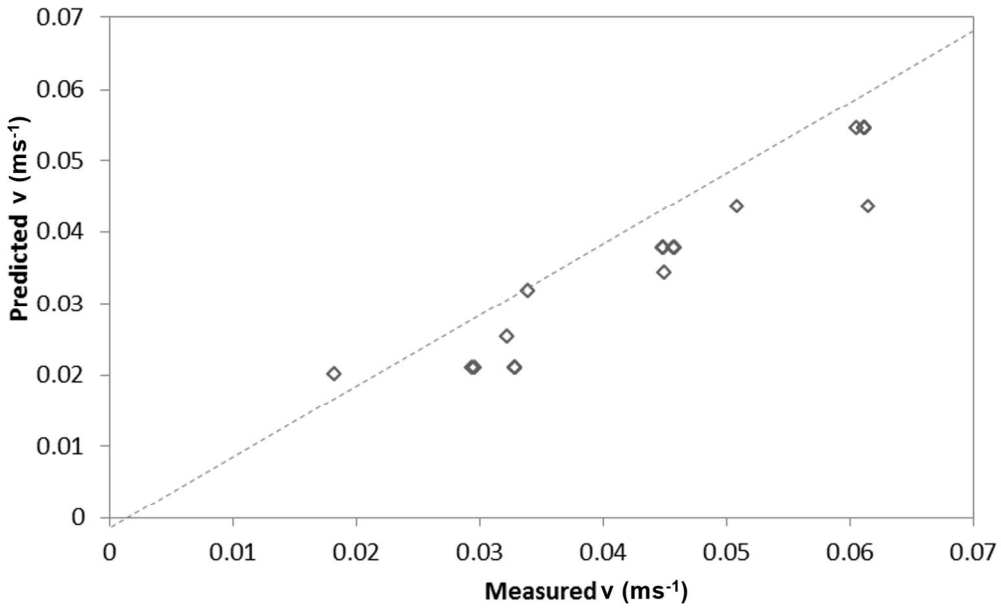

Figure 11, Measured (CFD) vs predicted velocity along the Laboratory trap seal at 2Hz (time: 0.125s) R^2 = 0.9163

205x122mm (192 x 192 DPI)

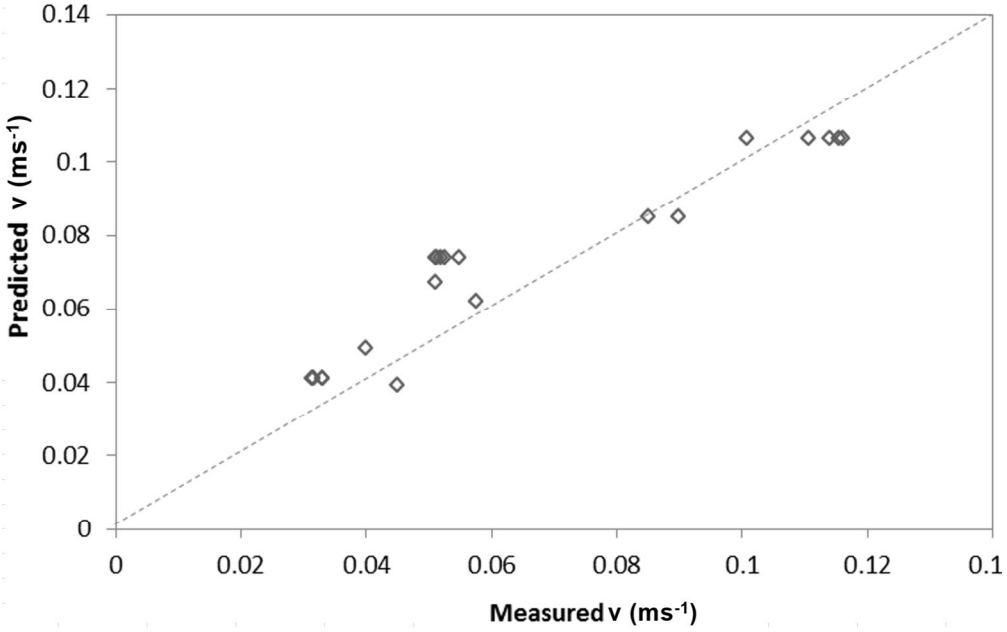

Figure 12, Measured (CFD) vs predicted velocity along the Commercial trap seal at 2Hz (time: 0.125s). R^2 = 0.8948

202x128mm (192 x 192 DPI)

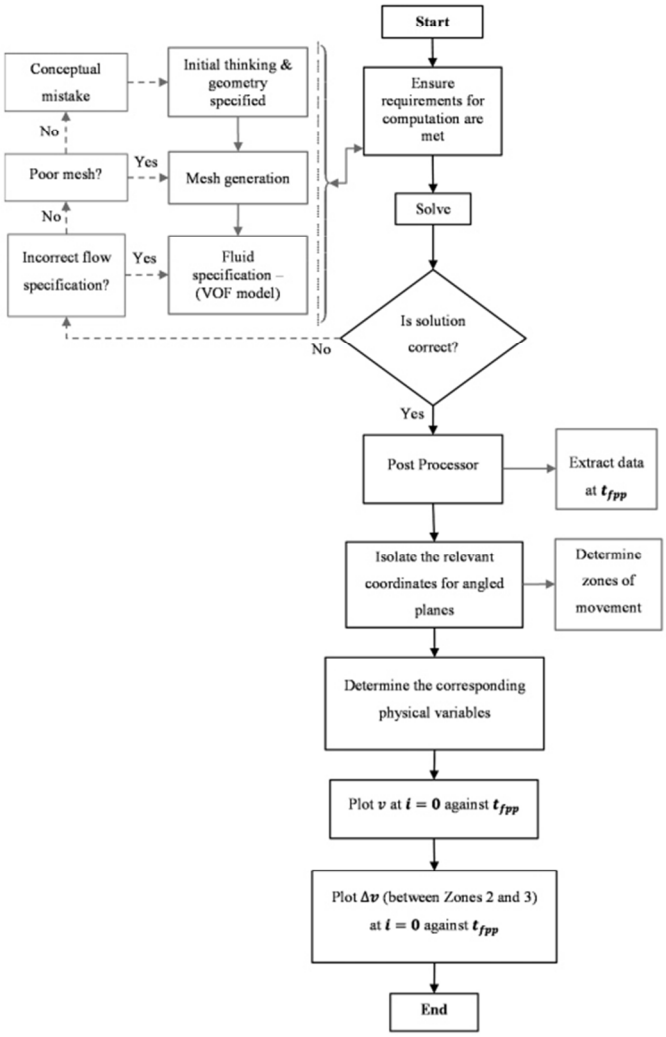

Figure 13, Methodology flowchart for boundary condition development of the water trap seal.

203x235mm (96 x 96 DPI)

Figure 14

Figure 14, Observation of the displacement of water in the appliance trap in the Heriot-Watt University drainage laboratory.

152x111mm (96 x 96 DPI)

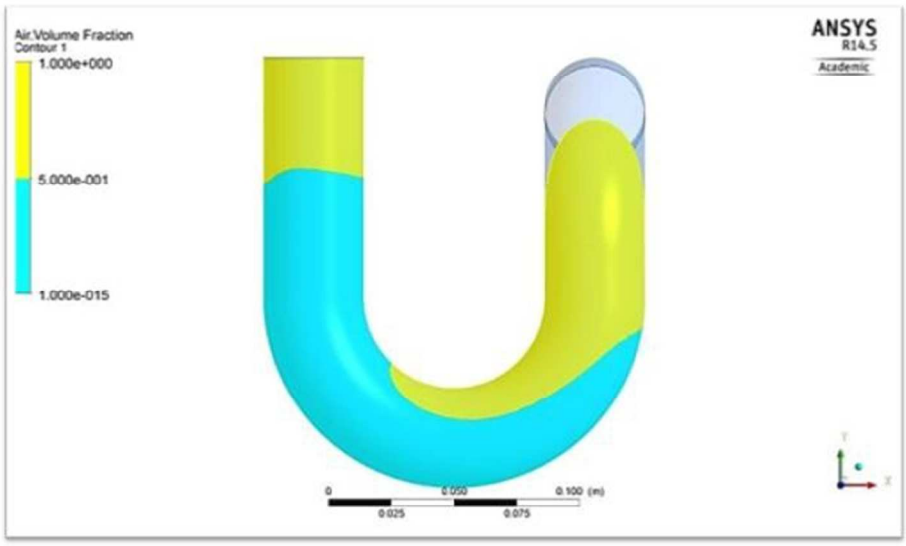

Figure 15

Figure 15, Air volume fraction across the XY plane (Z=0) in the laboratory appliance water trap at 0.5s when an applied 1Hz pressure transient.

177x114mm (96 x 96 DPI)

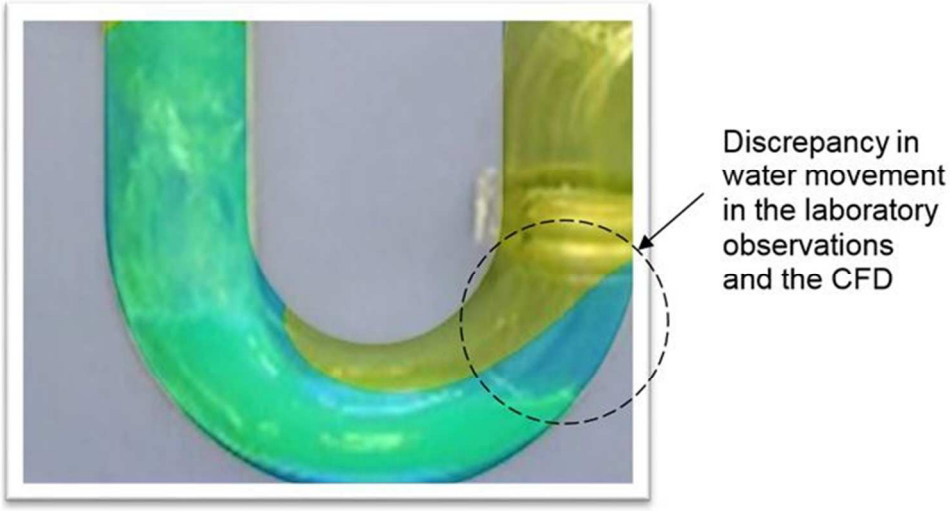

Figure 16

Figure 16, Overlay of the laboratory observation image and the VF results of the appliance trap seal from ANSYS CFX

190x118mm (96 x 96 DPI)

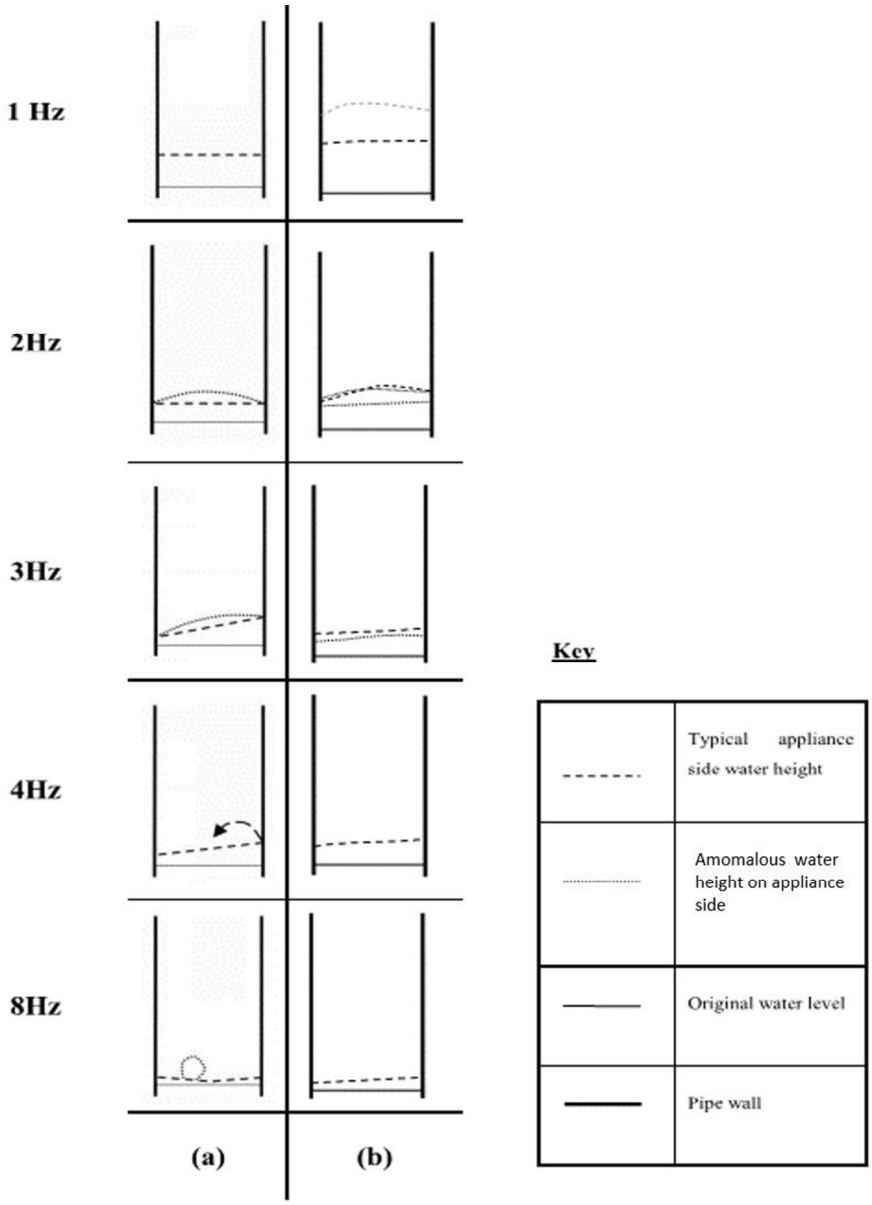

Figure 17, Representative sketches of the water oscillations for each tested frequency (a) Measured at 38mm water trap depth, Beattie (2007), (b) Predicted using ANSYS CFX at 38mm water trap depth

109x144mm (192 x 192 DPI)

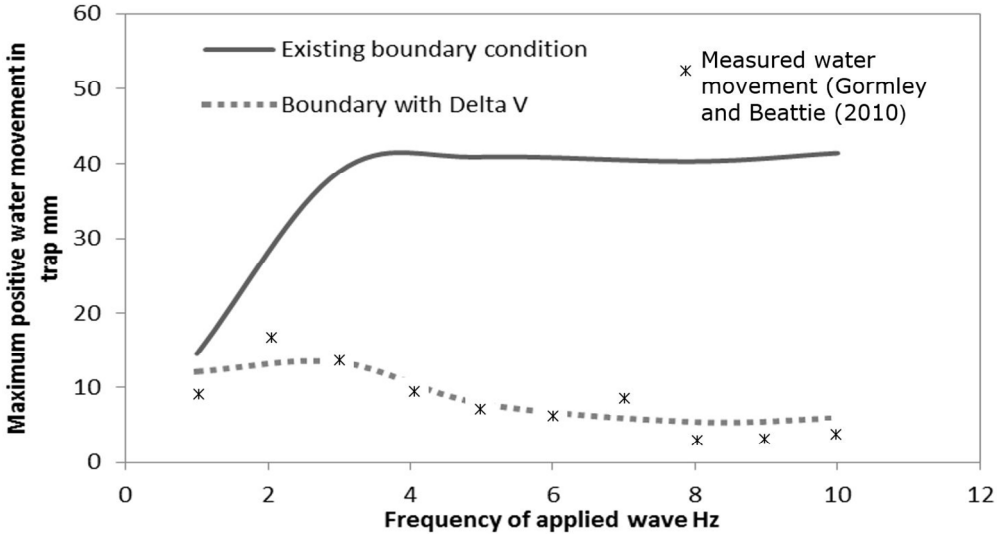

Figure 18, Comparison of water trap seal movement from predictions based on the existing boundary condition, the new delta v boundary condition and measured data from Gormley and Beattie16

194x105mm (192 x 192 DPI)